Estimating Lumbar Spine Loading When Using Back-Support Exoskeletons in Lifting Tasks

Saman Madinei[a], Maury A. Nussbaum[a]

[a]Department of Industrial and Systems Engineering, Virginia Tech, Blacksburg, VA 24061, USA

CORRESPONDING ADDRESS: Maury A. Nussbaum
Department of Industrial and Systems Engineering,
Virginia Tech, 250 Durham Hall (0118), Blacksburg, VA 24061, USA.
Phone: (540) 231-6053. E-mail: nussbaum@vt.edu. Fax: (540) 231-3322

Acknowledgment: all authors have made substantial contributions to all of the following: (1) the conception and design of the study, or acquisition of data, or analysis and interpretation of data, (2) drafting the article or revising it critically for important intellectual content, and (3) final approval of the version to be submitted.

Abstract

Low-back pain (LBP) continues as the leading cause of work-related musculoskeletal disorders, and the high LBP burden is attributed largely to physical risk factors prevalent in manual material handling tasks. Industrial back-support exoskeletons (BSEs) are a promising ergonomic intervention to help control/prevent exposures to such risk factors. While earlier research has demonstrated beneficial effects of BSEs in terms of reductions in superficial back muscle activity, limited evidence is available regarding the impacts of these devices on spine loads. We evaluated the effects of two passive BSEs (BackX™ AC and Laevo™ V2.5) on lumbosacral compression and shear forces during repetitive lifting using an optimization-based model. Eighteen participants (gender-balanced) completed four minutes of repetitive lifting in nine different conditions, involving symmetric and asymmetric postures when using the BSEs (along with no BSE as a control condition). Using both BSEs reduced estimated peak compression and anteroposterior shear forces (by ~8-15%). Such reductions, however, were task-specific and depended on the BSE design. Laevo™ use reduced mediolateral shear forces during asymmetric lifting (by ~35%). We also found that reductions in composite measures of trunk muscle activity may not correspond well with changes in spine forces when using a BSE. These results can help guide the proper selection and application of BSEs during repetitive lifting tasks. Future work is recommended to explore the viability of different biomechanical models to assess changes in spine mechanical loads when using BSEs and whether reasonable estimates would be obtained using such models.

Keywords: Low-Back Pain, Wearable Assistive Devices, Computational Biomechanics, AnyBody™ Modeling System, Musculoskeletal Modeling

1. Introduction:

Work-related musculoskeletal disorders (WMSDs) remain prevalent, with the back most often affected (BLS, 2019). This prevalence is attributed largely to physical risk factors prevalent in manual material handling (MMH) tasks, including forceful exertions, repetitive lifting and bending, and sustained/prolonged non-neutral postures (da Costa & Vieira, 2010; Hoogendoorn et al., 2000). Back-support exoskeletons (BSEs) are a new ergonomic intervention to reduce physical demands on the spine (De Looze et al., 2016). Passive BSEs, requiring no actuators or power supply, are of specific interest here, due to their cost-efficiency, ease of implementation, and predominance in the commercial market.

Existing evidence supports the potential for passive BSEs to reduce physical demands in the low back, but most earlier studies concluded this only via reductions in superficial back muscle activity (e.g., Alemi et al., 2019; Lamers et al. (2018); Madinei et al., 2020; Näf et al., 2018). Spine loads, however, are also influenced by deep trunk muscles and passive tissues (Bazrgari & Shirazi-Adl, 2007) as well as segmental kinematics and external loads. Consequently, reductions in back muscle activity, evidenced via electromyography (EMG), may not necessarily imply a reduction in spine loading.

BSE effects on spine compression forces have been assessed during static holding and dynamic lifting tasks using EMG-assisted biomechanical models. Findings indicate that BSEs reduce spine compression by ~15-20% during lifting tasks (Koopman, Näf, et al., 2020; Koopman, Kingma, et al., 2020; Schmalz et al., 2021), but such reductions vary substantially between different exoskeleton designs (Kingma et al., 2022). We reported an assessment of two passive BSEs during symmetric and asymmetric repetitive lifting tasks (Madinei et al., 2020), finding 9-20% reductions in trunk extensor muscle activities with minimal changes in lifting behavior. We

67 did not report whether there were similar changes in spine reactions forces. Thus, our first objective
68 was to estimate lumbar spine loads during the tasks. We hypothesized that using both BSEs would
69 reduce spine loads (i.e., lumbosacral compression and shear), though to differing extents across
70 task conditions.

71 In contrast to earlier studies, an EMG-assisted model was not used here. We could not
72 easily measure the activity of all trunk muscles of interest with the BSEs tested, since the BSE
73 structures and padding interfered with surface EMG sensors. We instead used an optimization-
74 based musculoskeletal model in the AnyBody Modeling System (AMS). However, using detailed
75 biomechanical models to assess spinal loading can be challenging, given the additional expertise
76 and experimental effort required (e.g., for model calibration and EMG normalization). Thus, our
77 second objective was to determine if BSE effects on spine loads are correlated with EMG from
78 accessible trunk muscles. A high correspondence would suggest the feasibility of simpler field-
79 based estimates of BSE effects. We expected that BSE effects on spinal loads would not strongly
80 or consistently correspond with changes in superficial back muscle activity, given that the latter
81 has only a partial role contributing to spine loads.

82

83 **2. Methods**

84 2.1. Experimental design and procedures:

85 We used data obtained from an earlier study; complete details are provided in Madinei et
86 al. (2020) and are only summarized here. Participants (9 females and 9 males) performed free-
87 style repetitive lifting in several combinations of *Intervention* and *Task Condition*. *Intervention*
88 included three levels: a control (unassisted) condition and two BSEs (BackX™ AC –
89 https://www.suitx.com/backx; and Laevo™ V2.5 – https://www.laevo-

exoskeletons.com/en/laevo-v2-1). There were three *Task Conditions* (Figure A1): 1) symmetric lowering/lifting to/from mid-shank (Sym_Ground) and 2) knee level (Sym_Knee), and 3) asymmetric lowering/lifting to/from knee height at 90º to the right of the mid-sagittal plane (Asy_Knee). All conditions started in a standing posture with the box at waist height. Participants completed repetitive lowering/lifting using a wooden box (40 x 25 x 23 cm; 4 cm handle clearance), which was set to 10% of individual body mass. Each task condition lasted four minutes, at a pace of 10 lower/lift cycles per minute, for a total of 40 cycles. Boxes were moved to/from a height-adjustable table and target locations that were marked using wooden blocks; horizontal distances between the target location centers were controlled at 25 and 50 cm in the symmetric and **asymmetric** conditions, respectively. Participants could freely choose their lifting style and feet locations, but feet locations were kept consistent within a given condition.

Whole-body segmental kinematics were monitored using an inertial motion capture system (MVN Awinda, Xsens Technologies B.V., the Netherlands: 60 Hz). Surface electromyography (EMG: 1.5 kHz) was obtained bilaterally from the thoracic erector spinae (TES), iliocostalis lumborum (ILL), rectus abdominis (RA), and external oblique (EO). EMGs were subsequently normalized to peak values measured in maximum voluntary isometric exertions for each muscle group (trunk flexion, extension, and bidirectional axial rotation).

2.2. Model setup:

An anatomically-detailed spine model in the AnyBody™ Modeling System (AMS: Version 7.3, AnyBody Technology, Aalborg, Denmark) was employed, using the AnyBody Modeling Repository (AMMR V.2.3.3), to estimate lumbosacral compression and shear forces. The model consisted of seven rigid segments (pelvis, five lumbar vertebrae, and thorax) with six

113 ball-and-socket lumbar and thoracolumbar joints. This model accounts for nonlinear passive
114 properties of the ligamentous spine, dynamic characteristics of the trunk, detailed muscle
115 architecture, wrapping of the global extensor muscles, and satisfaction of equilibrium at all spinal
116 levels and directions (De Zee et al., 2007; Han et al., 2012; Hansen et al., 2006). Earlier reports
117 have supported the ability of the AMS spine model to estimate spine loads during static
118 holding/bending (Rajaee et al., 2015; Rasmussen et al., 2009) and dynamic lifting tasks (Bassani
119 et al., 2017; Larsen et al., 2020). High correlations were also reported between model-based
120 estimates and gold-standard *in vivo* measurements (Wilke et al., 2001) of intradiscal pressure over
121 a moderate range of trunk bending and twisting.

122 Full body kinematics from our earlier study were exported from Xsens MVN Studio as
123 .bvh files and imported into AMS, in which a linked-segment model with 44 degrees-of-freedom
124 was reconstructed (Larsen et al., 2020). We used an established approach involving virtual markers
125 to match the linked-segment model with the musculoskeletal model, minimizing linear distances
126 between virtual markers and the musculoskeletal model (Andersen et al., 2010; Skals, Rasmussen,
127 et al., 2017; Karatsidis et al., 2019). Ground reaction forces were predicted using a method
128 described previously (Fluit et al., 2014; Karatsidis et al., 2019; Skals, Jung, et al., 2017). In brief,
129 25 dynamic contact elements were attached under each foot. Each contact element consisted of
130 five uniaxial force actuators to generate a positive normal force, as well as positive and negative
131 anteroposterior and mediolateral static friction forces. Individual actuation of each contact force
132 actuator was then computed as part of the muscle recruitment problem.

133 Muscle activations and internal reaction forces were computed through an inverse dynamic
134 analysis, by minimizing the sum of quadratic muscle stress (Damsgaard et al., 2006; Rasmussen
135 et al., 2001). Participant body mass, stature, and other anthropometric measures (e.g., trunk length,

shoulder width, hip width, arm span) were used to scale body segment masses and lengths in the AMS. A mechanical interface for each BSE was created in the AMS platform, consisting of a torso frame hinged to two leg frames at the hip joint (Figure 1). Chest plate length was adjusted based on each participant's xiphoid process, and leg frame lengths were adjusted based on BSE dimensions. BSE frames were connected to the body at the xiphoid process, hip joints, and thighs (the specific location on the thighs depended on participant anthropometry, given the fixed length of the BSE thigh frames). Kinematics of the torso and leg frames were constrained to follow participant torso and hip motions, respectively. Torque profiles of each BSE were applied to revolute (hinge) joints created in AMS; these joints were created by the torso frame and the leg frame nodes, merging at the hip joint of the human body model.

The mechanical behavior of each BSE (i.e., torque vs. angle relationship) was measured using a dynamometer (Humac Norm, CSMi, MA), using procedures presented elsewhere (Madinei et al., 2022). Briefly, a flexible mannequin with hinge joints at the hips was used to mimic hip flexion/extension with the BSE was attached. Hip torque was recorded in the continuous passive model at 100 Hz. BSE torque profiles were derived as a function of angular position and velocity to model the assistive torque provided by the BSEs in the AMS.

2.3. Data processing and outcome measures

Given that processing all 40 cycles of each condition was excessively time-consuming, our analysis focused on the 10th and 30th lowering/lifting cycles in each condition. Three-dimensional reaction forces at the lumbosacral (L5/S1) intervertebral joint were extracted from the AMS in a local coordinate system, specifically axial compression (F_{COMP}), anteroposterior shear (F_{AP}), and mediolateral shear (F_{ML}). Given symmetry, all F_{ML} data were converted to absolute values. Peak

159 (95th percentile) values were derived as outcome measures. As in our earlier analysis (Madinei et
160 al., 2020), outcome measures were obtained separately in the lowering and lifting phases.

161

162 2.4. Statistical Analyses

163 Separate three-way, mixed-factor analyses of variance (ANOVAs) were used to assess the
164 effects of *Intervention*, *Task Condition*, and *Gender* on estimated peak spine forces. Since initial
165 analysis indicated no differences between the two cycles (p values ~0.8-0.9), we did not include
166 in the final ANOVA models. Presentation orders of *Task Condition* and *Intervention* were included
167 as blocking factors. Parametric model assumptions were assessed (e.g., normality of residuals and
168 equality of variances) and dependent variables violating these assumptions were transformed using
169 deterministic mathematical functions. Statistical significance was concluded when $p < 0.05$, and
170 effect sizes were estimated using eta-squared (η^2). Significant interaction effects were explored
171 using simple-effects testing, and *post hoc* paired comparisons were completed using the Tukey-
172 Kramer procedure where relevant. Given the study goals, the subsequent presentation of results
173 and the discussion emphasizes the main and interaction effects of *Intervention*.

174 We further explored the feasibility of using measured muscle activity to estimate changes
175 in simulated spinal loads when using the BSEs. We first obtained composite metrics of muscle
176 activity as has been done in prior work (Frost et al., 2009; Graham et al., 2009; Madinei et al.,
177 2020; Potvin et al., 1990). Such metrics were used since EMG from a single muscle is unlikely to
178 be highly correlated with spine loading, given the complexity and indeterminacy of the lumbar
179 musculoskeletal system. The first metric captured activity of the monitored trunk extensor muscles
180 (TEM), the major agonists, and was calculated as the sum of the peak (95th percentile) levels of
181 the bilateral iliocostalis lumborum and thoracis erector spinae muscles. Total trunk muscle (TTM)

activity was the second metric, obtained as the sum of normalized activity levels across the eight muscles monitored, and which included trunk muscle coactivity. We then derived relative changes in these metrics, along with changes in the estimated peak (95th percentile) spine loads, by comparing changes resulting from BSE use relative to the control (no EXO) condition. We initially explored the linear correlations between the metrics of muscle activity and the simulated forces across participants, and separately for each of the 12 combinations of *Intervention*, *Task Condition*, and *Gender*. In a subsequent analysis, we collapsed the data by averaging across participants in each of the 6 *Intervention* x *Task Condition* combinations, then examining correlations across the six combinations. Pearson correlation coefficients (r) were obtained as outcome measures.

3. Results

3.1. Spine Reaction Forces

ANOVA results for each outcome measure are summarized in Table A1 (Appendix). *Intervention* main effects were significant for F_{COMP} and F_{AP}. Using the BackX™ significantly reduced both of these reaction forces, respectively by 13.3 and 15.1% during the lowering phase, and by 8.2 and 8.5% during the lifting phase (Figure 2). Laevo™ use also led to significant reductions in F_{COMP} and F_{AP}, respectively by 9.5 and 10.6%, but only during the lowering phase (Figure 2).

There was a significant *Intervention* × *Task Condition* effect on F_{ML} during both the lowering and lifting phases. Specifically, *Task Condition* was significant for all three *Interventions* ($p < 0.0001$), but the effect of *Intervention* was only significant for Asy_Knee ($p < 0.0001$). F_{ML} decreased significantly when using the Laevo™ in the Asy_Knee condition, by 34.5% during the lowering phase and by 30.5% during the lifting phase (Figure 3).

3.2. Correlation coefficients

When analyzed separately within each combination of *Intervention* and *Task Condition*, most correlation coefficients were small ($|r|$< ~0.3) and not statistically significant (Table A2). Furthermore, visual inspection did not reveal any clear or consistent relationships between the estimated spine forces and metrics of muscle activity. After averaging across participants, however, the correlations were generally higher (Table 1). Strong correlations (r > ~0.8) were found for F_{COMP} among females, which were statistically significant during both lowering and lifting. Moderate correlations (r > ~0.6) were found among females for F_{AP}, although this was only significant during lowering. Small-to-moderate correlations (~0.2 < $|r|$ < ~0.5) were obtained for males for both F_{COMP} and F_{AP}, although none were statistically significant. Additional results from the correlation analyses are provided in Figure A1.

4. Discussion

4.1. Spine reaction forces

Earlier studies of passive back-support have demonstrated reductions in low back muscle activity, yet evidence is lacking on whether there are comparable effects on spine reaction forces (compression and shear). We hypothesized that spine loads would be reduced in some task conditions using two different BSEs. Estimates obtained using the AMS supported this hypothesis overall, but also indicated that reductions were task-specific and dependent on BSE design. Specifically, BackX™ use led to ~8-13% reductions in F_{COMP} and ~8-15% reductions in F_{AP} depending on the lifting phase. Using Laevo™ resulted in ~10% reductions in both F_{COMP} and

227 F_{AP} only during the lowering phase. Laevo™ use also reduced F_{ML} in the Asy_Knee condition, by
228 34.5 and 30.5% during the lowering and lifting phases, respectively.

229 Larger reductions in spine loads with BackX™ vs Laevo™ use likely resulted from the
230 higher support settings provided by the former (Madinei et al., 2022). BackX™ provides respective
231 torques up to 14.7 and 24.8 Nm in the low and high support settings during flexion, and 11.3 and
232 19.2 Nm during extension. Respective values for the Laevo™ are 7.9 and 9.7 Nm during flexion,
233 and 5.3 and 6.4 Nm during extension. Further, participants often preferred higher support settings
234 when using the BackX, which was seen with the Laevo™. Our estimates of changes in spine loads
235 are consistent overall with our earlier findings (Madinei et al., 2020), wherein we observed larger
236 reductions in trunk extensor muscle activity and total trunk muscle activity when using the
237 BackX™. Our current results also agree with other studies of BSEs during repetitive lifting tasks,
238 which found 10 - 20% decreases in estimated spine compression (Koopman, Kingma, et al., 2020;
239 Koopman, Näf, et al., 2020; Schmalz et al., 2021).

240 We found larger reductions in spine compression and shear forces during the lowering vs.
241 the lifting phase for either BSE, consistent with our earlier report of larger reductions in trunk
242 extensor muscle activity and the sum of trunk muscle activity during lowering vs. lifting (Madinei
243 et al., 2020). We suggest that the increased benefit while lowering is due to hysteresis present in
244 the torque generation mechanisms of both BSEs. As noted above, torque outputs generated by both
245 BSEs are greater during trunk flexion than extension, and Koopman et al. (2019) reported a similar
246 effect earlier for the Laevo™.

247 We found a significant decrease in F_{ML} during asymmetric lifting when using the Laevo™,
248 which might have resulted from kinematic changes caused by using this BSE. As we indicated
249 earlier for the dataset analyzed here (Madinei et al., 2020), Laevo™ use decreased lumbar axial

250 range-of-motion (ROM), by up to ~23%. It also decreased axial angular velocity, by up to ~14%
251 compared to using the BackX™ and ~12% with no BSE. Given that changes in trunk posture and
252 movement speed are directly associated with the mechanical loads on the spine (Davis & Marras,
253 2000; Lavender et al., 2003), these reductions in trunk kinematics likely contributed to the decrease
254 in F_{ML} during asymmetric lifting.

255

256 4.2. Can BSE-induced changes in spine loads be estimated from EMG?

257 As noted above, we did not use an EMG-based modeling approach to estimate spine loads
258 since collecting surface EMG was not feasible for some muscles. We thus explored the feasibility
259 of estimating *changes* in simulated spinal loads when using a BSE from *changes* in composite
260 measures of muscle activity. Our results build on earlier evidence that simple measures of muscle
261 activity might indirectly estimate spinal loads. For example, Potvin et al. (1990) showed the
262 efficacy of EMG recordings from both thoracic and lumbar portions of the erector spinae muscles
263 in estimating dynamic lumbar compressive forces. Graham et al. (2009) used the same method to
264 assess low back demands when using a wearable assistive device (the "PLAD") during a repetitive
265 lifting task. A similar approach was adopted by Mientjes et al. (1999), who found moderate-to-
266 high correlations between normalized trunk muscle activity and spine compression forces, but only
267 for tasks involving minor axial moments.

268 Although we found no significant correlations between composite measures of muscle
269 activity and changes in spine forces at the individual level, noticeable correlations were found at
270 the group level. Changes in back muscle activity correlated reasonably well with relative changes
271 in spine compression and anteroposterior shear forces for female participants. Female participants
272 also experienced larger reductions in trunk muscle activity when using either BSE compared to

273 males (by 22.4% vs. 16.5% with BackX™; and by 11.5% vs. no change with Laevo™). We
274 speculated earlier (Madinei et al., 2020) that the latter outcome was partially due smaller torso
275 mass, since both genders selected comparable BSE support settings. Further, females overall had
276 larger (albeit non-significant) changes in spine loads using a BSE (Figure A1). These gender
277 differences in the effects of BSE use may account for why the noted correlated were higher among
278 females.

279 Our results confirm our initial expectation that changes in spine forces may not necessarily
280 correspond with changes in metrics of back muscle activity, and are perhaps not surprising given
281 that the latter has only a partial role contributing to resultant spine loads in some postures.
282 Practically, these results imply that composite measures of muscle activity may not have consistent
283 utility in estimating changes in spine forces resulting from BSE use, and thus, invalid conclusions
284 could be reached if investigators rely only on surface EMG measures to assess the impacts of BSEs
285 on spine loads. Further investigation, however, is needed to compare the composite measures of
286 muscle activity with other biomechanical models.

287 Indeed, earlier work has employed diverse musculoskeletal models for both exoskeleton
288 design and evaluation (e.g., de Kruif et al., 2017; Serrancolí et al., 2019; Tröster et al., 2020).
289 Several studies have used EMG-driven models to assess BSE effects on spine loads (Koopman,
290 Kingma, et al., 2020; Koopman, Näf, et al., 2020; Kingma et al., 2022) while others have employed
291 human simulation methods (e.g., Constantinescu et al., 2016; Marinou et al., 2021). Our current
292 approach builds more directly on the work of Cho et al. (2012), who incorporated a CAD model
293 of a BSE into the AMS with mechanical and dynamic constraints. Motion capture from a single
294 subject was used to drive the model, similar to our approach, though these authors did not report
295 spine loads. Heydari et al. (2013) used the AMS to assess the effects of a soft BSE (exosuit) during

296 static trunk flexion, but also did not report spine reaction forces. More recently, Schmalz et al.
297 (2021) used the AMS to model a BSE, wherein fixed joints were used to define body contact
298 points, and Fritzsche et al. (2021) used the AMS to evaluate an arm-support exoskeleton during
299 overhead work, employing spherical and prismatic joints to connect the device to the body. There
300 are thus a variety of simple and more complex methods that can be used to include an exoskeleton
301 in a musculoskeletal model, and we suggest that future work is needed to evaluate the benefits and
302 limitations of these approaches, particularly when estimating the effects of exoskeleton use on
303 spine loads is of primary interest.

304 It is worth noting that comparisons of estimated muscle forces/activities with the empirical
305 measures obtained from Madinei et al. (2020) was not possible due to lack of one-to-one
306 correspondence of the muscles in each approach. For example, the extensor muscles in
307 AnyBody™ consisted of tens of distinct fascicles, while the muscle activities recorded in Madinei
308 et al. (2020) might involve crosstalk from multiple adjacent muscles, making it challenging to
309 correlate the model-based output values (muscle activity and/or force) with EMG recordings.

310

311 4.3. Limitations

312 Some limitations of the current study need to be noted. First, while the anatomical fidelity
313 of the AMS model has been reported (De Zee et al., 2007; Han et al., 2012; Hansen et al., 2006)
314 the model does rely upon a number of assumptions (e.g., rigid rib cage and thoracic spine, lumbar
315 discs treated as spherical joints) that affect estimated of spine loads. Nevertheless, the effects of
316 such assumptions has been suggested to be minimal (Ignasiak et al., 2016). Second, reconstructing
317 motion data from IMUs may introduce some errors, such as from soft-tissue artifact and
318 discrepancies between the Xsens linked-segment model and the AMS musculoskeletal model

319 (Damsgaard et al., 2006; De Zee et al., 2007). The magnitude of such errors is expected to be <6º
320 (Karatsidis et al., 2019), and these errors should not affect our comparisons between conditions
321 since the errors are not likely to vary substantially between conditions. Third, we predicted ground
322 reaction forces rather than measuring them directly (e.g., using a force platform); this approach
323 was used since we were interested in using a protocol that would be feasible for field
324 implementation. Any resulting errors were likely to be comparable across experimental conditions
325 and thus not a source of bias in comparing between conditions. **Furthermore, the accuracy of**
326 **this approach – using inertial motion capture and predicted ground reaction forces for**
327 **estimating spine joint reaction forces – was previously shown to be effective during dynamic**
328 **tasks including symmetrical and asymmetrical lifting with varying weight (Larsen et al.,**
329 **2020).** Fourth, and similar to earlier work (e.g., Koopman, Näf, et al., 2020), we neglected any
330 effect of BSE mass in inverse dynamic analyses, as it was unclear how the mass (< 4.5 kg) was
331 distributed over the body. Given that much of the mass is carried by the pelvis, any effect on spine
332 loading is likely limited. Fifth, forces at the hand-box coupling were not measured, and these forces
333 were instead modelled with additional contact elements. These forces, however, are more relevant
334 to improve the accuracy of the kinetic computations *above* the thorax, such as for shoulder and
335 elbow joint reaction forces (Larsen et al., 2020). Sixth, there is the potential for relative
336 displacement between an exoskeleton and body segments (e.g., Baltrusch et al., 2018), though we
337 did not measure or account for this in our modeling approach. Finally, it is unclear if the current
338 results will generalize to different populations (e.g., experienced or older workers).

339 In summary, we evaluated the impacts of two passive BSEs on lumbosacral compressive
340 and shear forces during symmetric and asymmetric repetitive lifting using an optimization-based
341 musculoskeletal model. Using both BSEs reduced peak compression and anteroposterior shear

342 forces (by ~8-15%). Such reductions, however, were task-specific and depended on the BSE
343 design. Laevo™ use also reduced mediolateral shear forces during asymmetric lifting (by ~35%).
344 Our findings further suggest that composite measures of muscle activity may not have consistent
345 utility in predicting changes in spine forces resulting from BSE use. These results can help guide
346 the proper selection and application of BSEs during repetitive lifting tasks. Future work is
347 recommended to explore the feasibility of other biomechanical models to quantify changes in
348 mechanical loads on the spine caused by using a BSE, and if reasonable estimates would be
349 obtained using such models. Additional work is needed to determine if spinal load reductions
350 estimated here are comparable in field settings and whether such changes are sufficient to help
351 reduce the risk of low-back WMSDs during lifting.

352

353 **References**

354 Alemi, M. M., Geissinger, J., Simon, A. A., Chang, S. E., & Asbeck, A. T. (2019). A passive
355 exoskeleton reduces peak and mean EMG during symmetric and asymmetric lifting.
356 *Journal of Electromyography and Kinesiology, 47*, 25-34.

357 Andersen, M. S., Damsgaard, M., MacWilliams, B., & Rasmussen, J. (2010). A computationally
358 efficient optimisation-based method for parameter identification of kinematically
359 determinate and over-determinate biomechanical systems. *Computer methods in*
360 *biomechanics and biomedical engineering, 13*(2), 171-183.

361 Baltrusch, S. J., van Dieën, J. H., van Bennekom, C. A. M., & Houdijk, H. (2018). The effect of
362 a passive trunk exoskeleton on functional performance in healthy individuals. *Applied*
363 *Ergonomics, 72*, 94-106.

364 Bassani, T., Stucovitz, E., Qian, Z., Briguglio, M., & Galbusera, F. (2017). Validation of the
365 AnyBody full body musculoskeletal model in computing lumbar spine loads at L4L5
366 level. *Journal of biomechanics, 58*, 89-96.

367 Bazrgari, B., & Shirazi-Adl, A. (2007). Spinal stability and role of passive stiffness in dynamic
368 squat and stoop lifts. *Computer methods in biomechanics and biomedical engineering,*
369 *10*(5), 351-360.

370 BLS. (2019). Employer-Reported Workplace Injury and Illness — 2018. *Bureau of Labor*
371 *Statistics, U.S. Department of Labor*.

Cho, K., Kim, Y., Yi, D., Jung, M., & Lee, K. (2012). *Analysis and evaluation of a combined human-exoskeleton model under two different constraints condition.* Paper presented at the International Summit on Human Simulation, St. Pete Beach, FL.

Constantinescu, C., Muresan, P. C., & Simon, G. M. (2016). JackEx: the new digital manufacturing resource for optimization of exoskeleton-based factory environments. *Procedia CIRP, 50*, 508-511.

da Costa, B. R., & Vieira, E. R. (2010). Risk factors for work- related musculoskeletal disorders: a systematic review of recent longitudinal studies. *American journal of industrial medicine, 53*(3), 285-323.

Damsgaard, M., Rasmussen, J., Christensen, S. T., Surma, E., & de Zee, M. (2006). Analysis of musculoskeletal systems in the AnyBody Modeling System. *Simulation Modelling Practice and Theory, 14*(8), 1100-1111.

Davis, K., & Marras, W. (2000). The effects of motion on trunk biomechanics. *Clinical Biomechanics, 15*(10), 703-717.

de Kruif, B. J., Schmidhauser, E., Stadler, K. S., & O'Sullivan, L. W. (2017). Simulation architecture for modelling interaction between user and elbow-articulated exoskeleton. *Journal of Bionic Engineering, 14*(4), 706-715.

De Looze, M. P., Bosch, T., Krause, F., Stadler, K. S., & O'Sullivan, L. W. (2016). Exoskeletons for industrial application and their potential effects on physical work load. *Ergonomics, 59*(5), 671-681.

De Zee, M., Hansen, L., Wong, C., Rasmussen, J., & Simonsen, E. B. (2007). A generic detailed rigid-body lumbar spine model. *Journal of biomechanics, 40*(6), 1219-1227.

Fluit, R., Andersen, M. S., Kolk, S., Verdonschot, N., & Koopman, H. F. (2014). Prediction of ground reaction forces and moments during various activities of daily living. *Journal of biomechanics, 47*(10), 2321-2329.

Fritzsche, L., Galibarov, P. E., Gärtner, C., Bornmann, J., Damsgaard, M., Wall, R., . . . Babič, J. (2021). Assessing the efficiency of exoskeletons in physical strain reduction by biomechanical simulation with AnyBody Modeling System. *Wearable Technologies, 2*, e6.

Frost, D. M., Abdoli-E, M., & Stevenson, J. M. (2009). PLAD (personal lift assistive device) stiffness affects the lumbar flexion/extension moment and the posterior chain EMG during symmetrical lifting tasks. *Journal of Electromyography and Kinesiology, 19*(6), e403-e412.

Graham, R. B., Agnew, M. J., & Stevenson, J. M. (2009). Effectiveness of an on-body lifting aid at reducing low back physical demands during an automotive assembly task: Assessment of EMG response and user acceptability. *Applied ergonomics, 40*(5), 936-942.

Han, K.-S., Zander, T., Taylor, W. R., & Rohlmann, A. (2012). An enhanced and validated generic thoraco-lumbar spine model for prediction of muscle forces. *Medical engineering & physics, 34*(6), 709-716.

Hansen, L., De Zee, M., Rasmussen, J., Andersen, T. B., Wong, C., & Simonsen, E. B. (2006). Anatomy and biomechanics of the back muscles in the lumbar spine with reference to biomechanical modeling. *Spine, 31*(17), 1888-1899.

Heydari, H., Hoviattalab, M., Azghani, M. R., Ramezanzadehkoldeh, M., & Parnianpour, M. (2013). Investigation on a developed wearable assistive device (WAD) in reduction lumbar muscles activity. *Biomedical Engineering: Applications, Basis and Communications, 25*(3), 1350035.

Hoogendoorn, W. E., Bongers, P. M., de Vet, H. C., Douwes, M., Koes, B. W., Miedema, M. C., . . . Bouter, L. M. (2000). Flexion and rotation of the trunk and lifting at work are risk factors for low back pain: results of a prospective cohort study. *Spine, 25*(23), 3087-3092.

Ignasiak, D., Ferguson, S. J., & Arjmand, N. (2016). A rigid thorax assumption affects model loading predictions at the upper but not lower lumbar levels. *Journal of biomechanics, 49*(13), 3074-3078.

Karatsidis, A., Jung, M., Schepers, H. M., Bellusci, G., de Zee, M., Veltink, P. H., & Andersen, M. S. (2019). Musculoskeletal model-based inverse dynamic analysis under ambulatory conditions using inertial motion capture. *Medical engineering & physics, 65*, 68-77.

Kingma, I., Koopman, A. S., de Looze, M. P., & van Dieën, J. H. (2022). *Biomechanical evaluation of the effect of three trunk support exoskeletons on spine loading during lifting*, Cham.

Koopman, Näf, M., Baltrusch, S. J., Kingma, I., Rodriguez-Guerrero, C., Babič, J., . . . van Dieën, J. H. (2020). Biomechanical evaluation of a new passive back support exoskeleton. *Journal of Biomechanics, 105*, 109795.

Koopman, A. S., Kingma, I., de Looze, M. P., & van Dieën, J. H. (2020). Effects of a passive back exoskeleton on the mechanical loading of the low-back during symmetric lifting. *Journal of biomechanics, 102*, 109486.

Koopman, A. S., Kingma, I., Faber, G. S., de Looze, M. P., & van Dieën, J. H. (2019). Effects of a passive exoskeleton on the mechanical loading of the low back in static holding tasks. *Journal of biomechanics, 83*, 97-103.

Lamers, E. P., Yang, A. J., & Zelik, K. E. (2018). Feasibility of a biomechanically-assistive garment to reduce low back loading during leaning and lifting. *IEEE Transactions on biomedical engineering, 65*(8), 1674-1680.

Larsen, F. G., Svenningsen, F. P., Andersen, M. S., De Zee, M., & Skals, S. (2020). Estimation of spinal loading during manual materials handling using inertial motion capture. *Annals of biomedical engineering, 48*(2), 805-821.

Lavender, S. A., Andersson, G. B., Schipplein, O. D., & Fuentes, H. J. (2003). The effects of initial lifting height, load magnitude, and lifting speed on the peak dynamic L5/S1 moments. *International Journal of Industrial Ergonomics, 31*(1), 51-59.

Madinei, S., Alemi, M. M., Kim, S., Srinivasan, D., & Nussbaum, M. A. (2020). Biomechanical assessment of two back-support exoskeletons in symmetric and asymmetric repetitive lifting with moderate postural demands. *Applied ergonomics, 88*, 103156.

Madinei, S., Kim, S., Park, J. H., Srinivasan, D., & Nussbaum, M. A. (2022). A novel approach to quantify the assistive torque profiles generated by passive back-support exoskeletons. *Journal of Biomechanics, 145*, 111363.

Marinou, G., Millard, M., Šarabon, N., & Mombaur, K. (2021). Comparing the risk of low-back injury using model-based optimization: Improved technique versus exoskeleton assistance. *Wearable Technologies, 2*, e13.

Mientjes, M. I., Norman, R. W., Wells, R. P., & McGill, S. M. (1999). Assessment of an EMG-based method for continuous estimates of low back compression during asymmetrical occupational tasks. *Ergonomics, 42*(6), 868-879.

Näf, M. B., Koopman, A. S., Baltrusch, S., Rodriguez-Guerrero, C., Vanderborght, B., & Lefeber, D. (2018). Passive back support exoskeleton improves range of motion using flexible beams. *Frontiers in Robotics and AI, 5*, 72.

Potvin, J., Norman, R., & Wells, R. (1990). *A field method for continuous estimation of dynamic compressive forces on the L4/L5 disc during the performance of repetitive industrial tasks.* Paper presented at the Proceedings of the Annual Conference of the Human Factors Association of Canada.

Rajaee, M. A., Arjmand, N., Shirazi-Adl, A., Plamondon, A., & Schmidt, H. (2015). Comparative evaluation of six quantitative lifting tools to estimate spine loads during static activities. *Applied ergonomics, 48*, 22-32.

Rasmussen, J., Damsgaard, M., & Voigt, M. (2001). Muscle recruitment by the min/max criterion—a comparative numerical study. *Journal of biomechanics, 34*(3), 409-415.

Rasmussen, J., de Zee, M., & Carbes, S. (2009). *Validation of a biomechanical model of the lumbar spine.* Paper presented at the Congress of the International Society of Biomechanics, ISB.

Schmalz, T., Colienne, A., Bywater, E., Fritzsche, L., Gärtner, C., Bellmann, M., . . . Ernst, M. (2021). A passive back-support exoskeleton for manual materials handling: Reduction of low back loading and metabolic effort during repetitive lifting. *IISE Transactions on Occupational Ergonomics and Human Factors, 10*(1), 7-20.

Serrancolí, G., Falisse, A., Dembia, C., Vantilt, J., Tanghe, K., Lefeber, D., . . . De Groote, F. (2019). Subject-exoskeleton contact model calibration leads to accurate interaction force predictions. *IEEE Transactions on Neural Systems and Rehabilitation Engineering, 27*(8), 1597-1605.

Skals, S., Jung, M. K., Damsgaard, M., & Andersen, M. S. (2017). Prediction of ground reaction forces and moments during sports-related movements. *Multibody system dynamics, 39*(3), 175-195.

Skals, S., Rasmussen, K. P., Bendtsen, K. M., Yang, J., & Andersen, M. S. (2017). A musculoskeletal model driven by dual Microsoft Kinect Sensor data. *Multibody System Dynamics, 41*(4), 297-316.

Tröster, M., Wagner, D., Müller-Graf, F., Maufroy, C., Schneider, U., & Bauernhansl, T. (2020). Biomechanical model-based development of an active occupational upper-limb

exoskeleton to support healthcare workers in the surgery waiting room. *International Journal of Environmental Research and Public Health, 17*(14), 5140.

Wilke, H.-J., Neef, P., Hinz, B., Seidel, H., & Claes, L. (2001). Intradiscal pressure together with anthropometric data–a data set for the validation of models. *Clinical Biomechanics, 16*, S111-S126.

498 Table 1. Correlation coefficients (*r* values) between relative changes in simulated spinal loads
499 and the corresponding changes in composite metrics of muscle activities (i.e., TEM= trunk
500 extensor muscles; TTM= total trunk muscles). Bold values indicate statistically significant
501 values.

502

503

504 Figure 1. Illustration of the BSE interface in the AnyBody™ Modeling System, consisting of a
505 torso frame hinged to two leg frames at the hip joint. External hand forces are indicated by
506 vertical blue lines applied to the palm joints.

507 Figure 2. *Intervention* effects on peak compression and anteroposterior shear forces at the L5/S1
508 intervertebral joint. Note that * denotes significant differences from the control condition (i.e., no
509 BSE), and error bars indicate 95% confidence intervals.

510 Figure 3. *Intervention* × *Task Condition* interaction effects on the peak mediolateral shear forces
511 at the L5/S1 intervertebral joint. Note that * denotes significant differences from the control
512 condition (i.e., no BSE), and error bars indicate 95% confidence intervals.
513

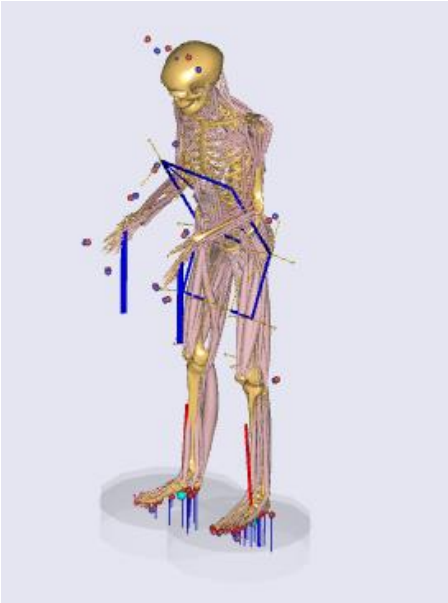

Figure 1. Illustration of the BSE interface in the AnyBody™ Modeling System, consisting of a torso frame hinged to two leg frames at the hip joint. External hand forces are indicated by vertical blue lines applied to the palm joints.

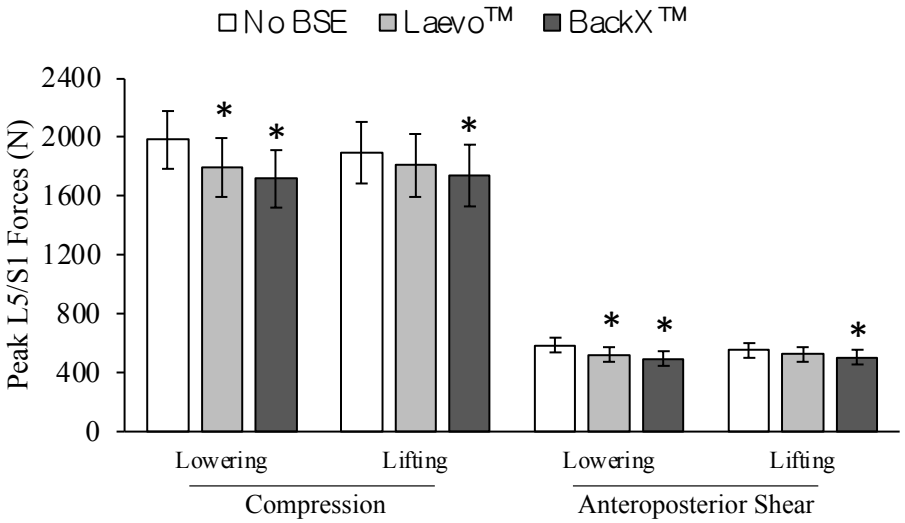

Figure 2. *Intervention* effects on peak compression and anteroposterior shear forces at the L5/S1 intervertebral joint. Note that * denotes significant differences from the control condition (i.e., no BSE), and error bars indicate 95% confidence intervals.

14

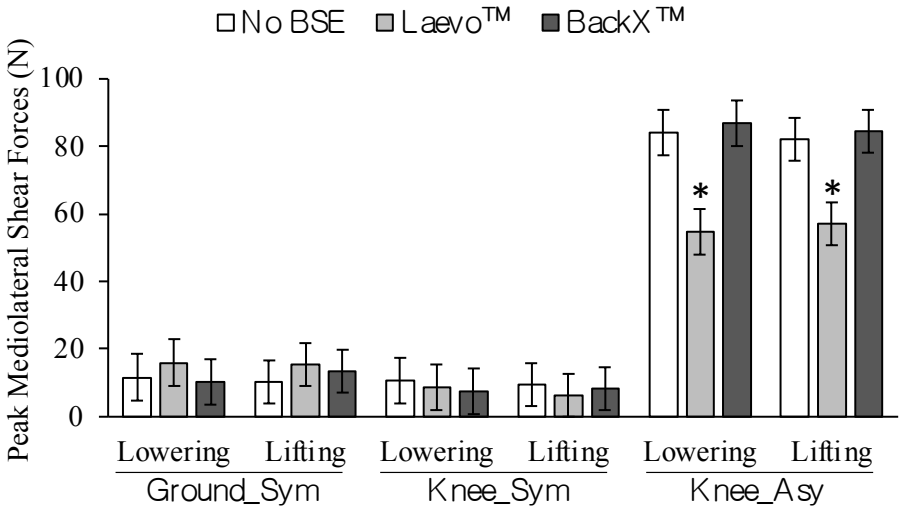

15

16 Figure 3. *Intervention × Task Condition* interaction effects on the peak mediolateral shear forces
17 at the L5/S1 intervertebral joint. Note that * denotes significant differences from the control
18 condition (i.e., no BSE), and error bars indicate 95% confidence intervals.

Table 1. Correlation coefficients (r values) between relative changes in simulated spinal loads and the corresponding changes in composite metrics of muscle activities (i.e., TEM= trunk extensor muscles; TTM= total trunk muscles). Bold values indicate statistically significant values.

		Composite measures			
		TEM		TTM	
Gender	Estimated Forces	Lowering	Lifting	Lowering	Lifting
Female	F_{COMP}	**0.900**	**0.784**	**0.887**	**0.782**
	F_{AP}	**0.897**	0.589	**0.878**	0.601
	F_{ML}	-0.184	-0.486	-0.163	-0.496
Male	F_{COMP}	0.346	-0.508	0.437	-0.470
	F_{AP}	0.456	-0.225	0.546	-0.181
	F_{ML}	-0.251	0.090	-0.407	-0.006